Microsecond electro-optic switching in nematic phase of ferroelectric nematic liquid crystal

Kamal Thapa^{ab}, Sathyanarayana Paladugu^a, Oleg D. Lavrentovich^{abc*}

^aAdvanced Materials and Liquid Crystal Institute, Kent State University, Kent, OH 44242, USA

^bDepartment of Physics, Kent State University, Kent, OH, 44241, USA

^cMaterials Science Graduate Program, Kent State University, Kent, OH 44242, USA

*olavrent@kent.edu; phone 1 330 672-4844; fax 1 330 672-2796; lavrentovichgroup.com

ABSTRACT

Nematic liquid crystals exhibit nanosecond electro-optic response to an applied electric field which modifies the degree of orientational order without realigning the molecular orientation. However, this nanosecond electrically-modified order parameter (NEMOP) effect requires high driving fields, on the order of 10^8 V/m for a modest birefringence change of 0.01. In this work, we demonstrate that a nematic phase of the recently discovered ferroelectric nematic materials exhibits a robust and fast electro-optic response. Namely, a relatively weak field of 2×10^7 V/m changes the birefringence by \approx 0.04 with field-on and -off times around 1 μ s. This microsecond electrically modified order parameter (MEMOP) effect shows a greatly improved figure of merit when compared to other electro-optical switching modes in liquid crystals, including the conventional Frederiks effect, and has a potential for applications in fast electro-optical devices such as phase modulators, optical shutters, displays, and beam steerers.

Keywords: Electro-optic response, field-induced birefringence, microsecond switching, ferroelectric nematic

1. INTRODUCTION

Nematic liquid crystals (NLCs) are widely used in electro-optic applications because of their intrinsic anisotropy of dielectric and optical properties [1]. Most applications rely on the Frederiks transition [2], in which an external electric field reorients the direction of average molecular orientation, called the director $\hat{\bf n}$. The detrimental feature of the Frederiks effect is its slow field-off relaxation, on the order of milliseconds [3]. When the field is switched off, the elastic nature of an NLC forces $\hat{\bf n}$ to return to its original orientation set up by the surface anchoring forces. The relaxation time $\tau_{\rm off}$ of this passive process is determined by the rotational viscosity γ_1 , elastic costant K, and thickness d of the cell, $\tau_{\rm off} = \frac{\gamma_1 d^2}{\pi^2 K}$. For typical $\gamma_1 = 0.1$ kg m⁻¹ s⁻¹, K = 10 pN, and d = 5 µm, one finds $\tau_{\rm off} \approx 25$ ms [3]. Many approaches have been developed over the years to speed up the relaxation; among these are the optimization of viscosity and elastic constants, development of the so-called dual frequency NLCs [3-8], polymer-layer-free alignment [9], design of gradient electric fields [10], and doping NLCs with various additives [11]. Still, the relaxation time of $\hat{\bf n}$ during the field-off state is in the millisecond or sub-millisecond range.

A different approach to the electro-optic switching is offered by the so-called nanosecond electrically-modified order parameter (NEMOP) effect, in which the applied electric field modifies the degree of orientational order but does not alter the orientation of $\hat{\mathbf{n}}$ [12-17]. The NEMOP effect was first demonstrated for an NLC CCN-47 with a negative dielectric anisotropy $\Delta \varepsilon = \varepsilon_{\parallel} - \varepsilon_{\perp} \approx -5$ [12, 14]; here the subscripts refer to the direction parallel and perpendicular to $\hat{\mathbf{n}}$, respectively. An electric field on the order of $\sim 10^8$ V/m applied perpendicularly to $\hat{\mathbf{n}}$ in a planar cell, causes a uniaxial-to-biaxial transformation of the order parameter and changes birefringence by ≈ 0.001 with the field-on $\tau_{\rm on}$ and $\tau_{\rm off}$ times being on the order of 10 ns [12, 14]. The reason for such a fast nanosecond switching is that the orientational order is altered at the molecular scale and does not involve collective realignment. Since the NEMOP effect is essentially a molecular-scale phenomenon, the amplitude and the relaxation times of birefringence change depend strongly on the details

of molecular structure. In particular, an order-of-magnitude enhancement of the birefringence change up to ≈ 0.01 was achieved in nematics HNG 715600-100, and HNG 705800-100 with negative dielectric anisotropy, $\Delta\epsilon \approx -10$, stronger than that of CCN-47 [13], and up to ≈ 0.02 when doped with highly polar molecules carrying a large transversal dipole [16]. The approach to modify the degree of orientational order can also be applied to nematics with $\Delta\epsilon > 0$ in a homeotropic cell, by applying the field along $\hat{\bf n}$ and using oblique incidence of light [15, 18]. In particular, nematics with $\Delta\epsilon \sim 100$ demonstrated a strong birefringence change ≈ 0.04 switched by a moderate field of 3×10^7 V/m, with $\tau_{\rm on} \approx \tau_{\rm off} \approx 10$ µs [18]. In the case of $\Delta\epsilon > 0$, the birefringence change is caused not only by the modification of the order parameter but also by the quenching of director fluctuation. The quenching is slower than the field-induced uniaxial-biaxial transformation. These prior experiments suggest that the performance of the electro-optical response of NLCs can be improved through searching for new materials with a molecular structure that favors a fast and large field-induced change of birefringence. Guided by this idea, in this work we explore the electro-optical switching of the nematic phase of ferroelectric nematic materials.

Ferroelectric nematic (N_F) materials have been synthesized and characterized only recently [19-24]. These materials are formed by rod-like molecules with large longitudinal electric dipoles ~10 D. The molecules align either in a paraelectric fashion, forming a conventional paraelectric nematic (N) phase, or in a polar fashion, with all the dipoles pointing in the same direction, forming N_F phase with a macroscopic spontaneous polarization **P** along $\hat{\bf n}$. The large dipole moments and strong polarity of the molecules yield a large $\Delta \varepsilon > 0$ [25], and strong birefringence [23, 26, 27] in both N and N_F phases. We demonstrate that the paraelectric nematic of the ferroelectric nematic mixture FNLC919 [26] with a large positive dielectric anisotropy $\Delta \varepsilon \approx (90-230)$ shows a strong change of birefringence ≈ 0.04 when a relatively weak electric field $\approx 2 \times 10^7$ V/m is applied parallel to $\hat{\bf n}$. The response is fast, with $\tau_{\rm on} \approx \tau_{\rm off} \approx 1$ µs. The performance of different electro-optical modes and materials can be compared by a commonly used figure of merit (FoM) = $\delta \Gamma_{\rm max}^2/\pi^2 \tau_{\rm off}$ [3, 28], where $\delta \Gamma_{\rm max} = d\delta n_{\rm max}$ and $\delta n_{\rm max}$ is the amplitude of the field-induced birefringence. For the conventional Frederiks transition, the maximum possible $\delta n_{\rm max}$ is the material birefringence $\Delta n = n_e - n_o \approx 0.2$, $\tau_{\rm off} \approx 25$ ms, so that for d = 5 µm, one finds FoM ≈ 4 µm²/s; here n_e and n_o are the extraordinary and ordinary refractive indices, respectively. The material explored in this work yields a much larger FoM $\approx 10^3$ µm²/s. The latter is also more than an order of magnitude higher than the FoM reported for a paraelectric N material GPDA200 with $\Delta \varepsilon \sim 100$ [18], thanks to a 10 times faster switching speed.

2. MATERIALS AND METHODS

The explored material FNLC919 (Merck KGaA) [26], shows the phase sequence: I – 82 °C - N - 46 °C - N_X - 32 °C - N_F upon cooling from the isotropic (I) phase, where N_X is an intermediate phase between the paraelectric N and the ferroelectric N_F phases. The frequency-dependent dielectric permittivities of the N are determined by measuring the capacitance of cells of thickness $d=55~\mu m$ with an LCR meter 4284A (Hewlett Packard). The dielectric permittivity ε_{\parallel} along $\hat{\bf n}$ is measured in a cell with a homeotropic alignment of $\hat{\bf n}$, set by spin-coated layers of polyimide SE5661 (Nissan Chemicals, Ltd.) whereas the perpendicular component, ε_{\perp} is measured in a planar cell with rubbed PI2555 coatings. The measured $\Delta \varepsilon = \varepsilon_{\parallel} - \varepsilon_{\perp}$ is positive and large, which increases from about 90 at 80 °C to about 230 at 70 °C. The electropical response is studied in the temperature range T=(70-80) °C of the N phase, using a flat cell of a thickness $d=5.2~\mu m$ assembled from two indium-tin-oxide (ITO) patterned glass substrates spin-coated with SE5661. The transparent patterned ITO electrodes have a low sheet resistance of 10 Ω/\Box and a small patterned area of 2 mm × 2 mm. The SE5661 coating sets homeotropic alignment in the N, Fig.1 (a).

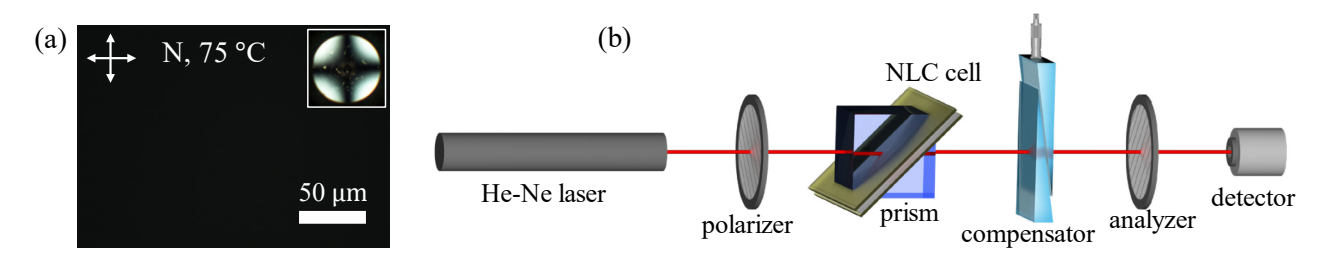


Figure 1. (a) Polarizing optical microscopy texture of a homeotropic cell ($d = 5.2 \,\mu\text{m}$) in the N phase (75 °C) with crossed polarizers; inset shows the conoscopy figure. (b) Experimental setup.

The electric field is applied along $\hat{\mathbf{n}}$ to change the degree of orientation but to avoid director reorientation. The field-induced birefringence δn is measured for an oblique 45° incidence of a He-Ne laser beam, $\lambda = 632.8$ nm, which passes through the LC cell and a Soleil-Babinet compensator, both in between two linear polarizers, Fig.1 (b). The N cell is sandwiched between two prisms inside a custom-made copper holder. The projection of $\hat{\mathbf{n}}$ onto the plane of the polarizer and analyzer, and the slow axis of the compensator are parallel to each other and make an angle of 45° with both polarization directions. The transmitted light intensity is measured using a photodetector TIA-525 (Terahertz Technologies, response time < 1 ns). Input voltage pulses of a duration 8 μ s are applied by a system of waveform generator WFG500 (FLC electronics), high direct current (DC) voltage source KEITHLEY 237 (Keithley), and pulse generator HV 1000 pulser (Direct Energy). The input voltage pulse and output photodetector signal are monitored by a digital oscilloscope TDS2014 (Tektronix). The temperature of the cell is controlled by a hot stage LTS120 and a controller PE94 (both Linkam) with an accuracy of 0.01°C.

The dynamics of the field-induced birefringence $\delta n(t)$ is calculated using the four-point measurement scheme, described in Ref. [18]. The technique uses four successive measurements of the transmitted intensities I_k , k = 1, 2, 3, 4, subjected to an identical electrical pulse at four different settings of the retardance Γ_k^{SB} of Soleil-Babinet compensator:

$$I_k(t) = \left[I_{\text{max}}(t) - I_{\text{min}}(t)\right] \sin^2\left\{\frac{\pi}{\lambda} \Gamma_k(t)\right\} + I_{\text{min}}(t) \tag{1}$$

where $\Gamma_k(t) = \Gamma_N(0) + \Gamma_k^{SB} + \delta\Gamma(t)$ is the total dynamic optical retardance of the system and $\Gamma_N(0)$ is the optical retardance of the N cell when there is no electric field. We select $\Gamma_k^{SB} = \lambda(m + k/4) - \Gamma_N(0)$, where m is an integer, in such a way that the initial intensities with zero field are maximum $I_2(0)$, minimum $I_4(0)$, and mean values $I_1(0) = I_3(0) = [I_2(0) + I_4(0)]/2$. For this selection, the field-induced birefringence is calculated as

$$\delta n(t) = \frac{\lambda}{2\pi d} \arg\{I_2(t) - I_4(t) + i[I_1(t) - I_3(t)]\}$$
 (2)

The switching-on $\tau_{\rm on}$ and switching-off $\tau_{\rm off}$ times are defined as the times within which $\delta n(t)$ changes between 10% and 90% of its maximum value $\delta n_{\rm max}$.

3. RESULTS AND DISCUSSION

The microsecond dynamics of the field-induced birefringence $\delta n(t)$ of the N cell is shown in Fig. 2 (a). The birefringence amplitude $\delta n_{\rm max}$ increases with the driving field, Fig.2 (b,d), and the temperature, see Fig. 2 (c) and the inset in Fig. 2 (d). The switching times $\tau_{\rm on}$ and $\tau_{\rm off}$ are around 1 μ s; the lowest value of the sum $\tau_{\rm on} + \tau_{\rm off} \approx 1.7~\mu s$ is achieved at 78 °C and $E = 19~V/\mu m$, Fig. 2 (e,f).

Table 1 compares the electro-optical performance of the studied N_F-forming material to the previously reported materials that do not form the N_F. The table shows the amplitude $\delta n_{\rm max}$ of the field-induced birefringence, switching speeds, required driving electric fields, and FoMs. In terms of the birefringence change, a close performance was recorded for a paraelectric N material GPDA200 [18] which yields $\delta n_{\rm max} \approx 0.04$ achieved at $E \approx 3 \times 10^7$ V/m with switching times ≈ 10 µs. In our FNLC919 material, a similar $\delta n_{\rm max} \approx 0.04$ is obtained at a somewhat lower field $E \approx 2 \times 10^7$ V/m, but with much shorter switching times ≈ 1 µs. In the enhanced NEMOP [16], switching times are even shorter ≈ 0.1 µs, but the birefringence change is weaker, $\delta n_{\rm max} \approx 0.02$, while the driving field is higher, $E \approx 2 \times 10^8$ V/µm.

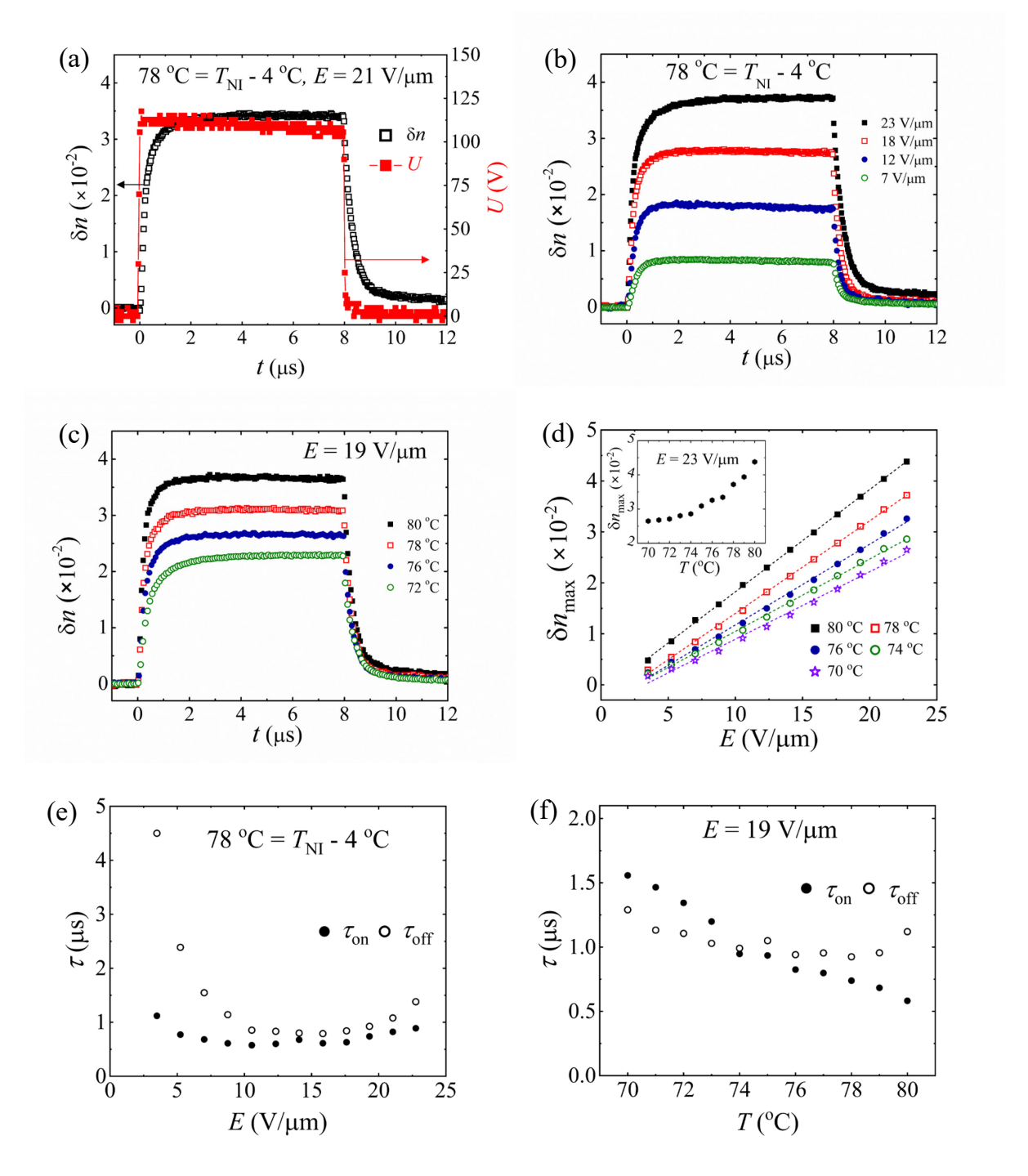


Figure 2. Microsecond electro-optic switching of birefringence in the N phase of the ferroelectric FNLC919. (a) Dynamics of birefringence $\delta n(t)$ in response to the applied voltage pulse U at 78 °C; (b) dynamics of $\delta n(t)$ at various voltages, 78 °C; and (c) at various temperatures, $E=19~\text{V/}\mu\text{m}$; (d) Amplitude δn_{max} of field-induced birefringence as a function of electric fields at various temperatures with the dashed lines showing the linear fittings and the inset image showing the temperature dependence of amplitude of field-induced birefringence at 23 V/ μ m. Switching times at various (e) electric fields at 78 °C and (f) temperatures at 19 V/ μ m.

Table 1. Field-induced birefringence in different electro-optic effects that do not involve director realignment; NEMOP stands for nanosecond electric modification of the order parameter; MEMOP stands for microsecond electric modification of the order parameter.

Effect	Material	Δε	<i>T</i> (°C)	E (V/m)	$\delta n_{ m max}$	$ au_{ m on}$	$ au_{ m off}$	FoM* (μm²/s)
NEMOP [13]	HNG715600-100	-12	23	1.7×10^{8}	0.013	30 ns	30 ns	1.3×10^4
Enhanced NEMOP [16]	HNG715600-100 doped with DPP (19 wt.%)	-14	23	1.9×10^{8}	0.020	130 ns	70 ns	1.4×10^4
MEMOP[18] in the paraelectric N material	GPDA 200	30 at 70 °C	72	2.8×10^7	0.038	7 μs	13 μs	2.8×10^{2}
MEMOP in the N phase of the N _F forming material	FNLC919	90	80	2.1×10^7	0.040	0.65 μs	1.3 μs	3.0×10^3

^{*} FoMs are calculated with $d = 5 \mu m$.

In electrically controlled liquid crystal-based optical retarders, the goal is to switch a sufficiently large optical retardance $\delta \Gamma_{\rm max}$, at least equal to half of the probing wavelength $\lambda/2$ within the shortest possible time. These features are characterized by FoM expressed as $\delta \Gamma_{\rm max}^2/\pi^2 \tau_{\rm off}$. The FOM of FNLC191 is on the order of $10^3 \, \mu m^2/s$ ($\delta n_{\rm max} = 0.04$, $d \approx 5 \, \mu m$, $\tau_{\rm off} \approx 1 \, \mu s$), which is one order of magnitude higher than the FoM of GPDA200 (FOM $\sim 10^2 \, \mu m^2/s$, $\delta n_{\rm max} = 0.04$, $d \approx 5 \, \mu m$, $\tau_{\rm off} \approx 10 \, \mu s$) [18], and is at least two to three orders of magnitude higher than the FoM of the conventional Frederiks effect, $\sim (1-10) \, \mu m^2/s$ [3, 28, 29]. Importantly, the demonstrated $\delta n \approx 0.04$ of the explored FNLC919 allows one to achieve a reasonably large retardance $\delta \Gamma \sim 400 \, nm$ in relatively thin 10 μ m cells.

In NLCs, the field-induced birefringence δn is caused by the modification of the uniaxial order parameter [14] and quenching of the director fluctuations [30, 31]. The modification of the uniaxial order parameter is proportional to the square of an electric field [14]. In our case, $\delta n_{\rm max}$ grows linearly with the field in the range (3 – 23) V/ μ m, Fig. 3 (d), indicating that the quenching of director fluctuations dominates over the modification of the uniaxial order parameter, similar to the previously reported effects in GPDA200 [18] and in 5CB [31]. As discussed in Ref. [18], the predominance of fluctuation quenching in a homeotropic N cell with $d=5~\mu$ m and $\Delta \varepsilon=100$, sets in at the fields above $E_{\rm fluct}=\beta/d\sqrt{\Delta \varepsilon}\approx 2~{\rm V}/\mu$ m, where $\beta\sim100~{\rm V}$ is parameter deduced from the numerical fitting of 5CB behavior. The field-induced birefringence change caused by the quenching of director fluctuations has been calculated as [14, 18],

$$\delta n_{\text{max}} \approx \frac{6k_B T \Delta n \sqrt{\varepsilon_0 \Delta \varepsilon}}{\sqrt{2} K_{\text{eff}}^{3/2}} E, \tag{3}$$

where T is the absolute temperature, $k_B = 1.38 \times 10^{-23}$ J/K is the Boltzmann constant, $\varepsilon_0 \approx 8.85 \times 10^{-12}$ F/m is the dielectric permittivity of free space, and $K_{\rm eff} = (4K_3)^{1/3}/(K_1^{-1} + K_2^{-1})^{2/3}$ is the effective elastic constant with K_1 , K_2 , and K_3 being the splay, twist, and bend elastic constants of the N, respectively. The last formula suggests that the smaller driving field causes the same $\delta n_{\rm max}$ in FNLC919 as compared to GPDA200 in Ref. [18], which can be attributed to a larger $\Delta \varepsilon$ of FNLC919. The data presented in Ref. [18] for GPDA200 with $\Delta \varepsilon \approx 30$ at about 2 °C below the NI phase transition yield the linear slope $\delta n_{\rm max}/E \approx 0.14$ µm/V. In FNLC919 with $\Delta \varepsilon \approx 90$ at the similar distance from the NI transition point, this slope is steeper, $\delta n_{\rm max}/E \approx 0.20$ µm/V, Fig. 3 (d). The ratio of slopes is $0.14/0.20 \approx 0.7$ which is close to the dielectric ratio $\sqrt{30}/\sqrt{90} \approx 0.6$. The higher dielectric anisotropy of FNLC919 allows one to use relatively weak driving fields (3-23) V/µm as compared to (3-35) V/µm in the case of GPDA200 to achieve the same $\delta n_{\rm max}$. The increase of $\delta n_{\rm max}$ with the temperature, inset of Fig. 3(d), can be explained by the growth of fluctuations with temperature.

The field-on switching time $\tau_{\rm on}(E)$ as a function of the applied field is nonmonotonous, strongly decreasing in the range $E = (3-15) \text{ V}/\mu\text{m}$ and somewhat increasing in the range $E = (15-23) \text{ V}/\mu\text{m}$. The decrease of $\tau_{\rm on}(E)$ is expected, as

the result of a stronger dielectric torque. The increase of $\tau_{\rm on}(E)$ is less clear; possible mechanisms are a formation of the field-induced polar order and dielectric memory, i.e., the dependence of the dielectric torque on the past and present values of the electric field when the rise time of the voltage pulse is comparable to the dielectric relaxation time [18, 32, 33]. The field-off time $\tau_{\rm off}(E)$ dependency is also nonmonotonous but much weaker, Fig.3 (e). As a function of increasing temperature, $\tau_{on}(T)$ decreases, which is expected since viscosity decreases. In contrast, $\tau_{off}(T)$ is nonmonotonous with an increase at higher temperatures. Since the field-off relaxation depends on both the viscous and elastic properties, this unusual behavior might be explained by a stronger decrease of the elastic constants with the temperature, as compared to the viscosity.

5. CONCLUSION

We demonstrate a microsecond electrically-modified order parameter (MEMOP) effect in the nematic phase of the ferroelectric nematic material FNLC919, in which the electric field on the order of 10⁷ V/m enhances the birefringence by $\delta n_{\rm max} \approx (0.01-0.04)$. We stress that the effect is explored in the N phase, which allows one to construct the homeotropic cells and apply the electric field along the director by using transparent electrodes on the bounding plates. This homeotropic geometry is hard, if at all possible, to reproduce in the N_F phase since the high electric polarization deposits a strong charge on the bounding plates; so far, no homeotropic alignment of the N_F has been reported. Linear dependence of $\delta n_{\rm max}$ on the field, E suggests that the main mechanism is the quenching of the director fluctuations. Compared to the NEMOP effect in conventional paraelectric NLCs [13, 16], the operating fields for FNLC919 are about one order of magnitude lower, and the field-induced birefringence changes are a few times stronger. The electro-optic response of FNLC919 is very fast, around 1 µs for both field-on and field-off switching. Overall, the FoM of the explored N material is two to three orders of magnitude higher than that of the conventional Frederiks effect [3, 29] and one order of magnitude higher than the previously reported MEMOP effect in the N material GPDA200 that does not form a ferroelectric N_F phase [18]. The FoMs of the NEMOP effects in Table 1 are higher than the FoM of FNLC919, mainly because the NEMOP switching times are shorter than 0.1 µs. The 1 µs MEMOP performance of FNLC919 fills the gap between the previously reported NEMOP and 10 µs MEMOP effects. Therefore, the electro-optics of the N phase based on ferroelectric nematic materials might find applications where the response time is not required to be shorter than 1 µs.

ACKNOWLEDGEMENTS

We thank Sergij V. Shiyanovskii for the useful discussions. We thank Merck KGaA, Darmstadt, Germany for providing us N_F material FNLC-919. The work was supported by NSF Grant ECCS-2122399.

REFERENCES

- [1] D.-K. Yang, and S.-T. Wu, [Fundamentals of liquid crystal devices] John Wiley & Sons, (2014).
- [2] A. Repiova, and V. Frederiks, "On the nature of the anisotropic liquid state of mater, J," Russian Phys. Chem. Soc, 59, 183 (1927).
- A. B. Golovin, S. V. Shiyanovskii, and O. D. Lavrentovich, "Fast switching dual-frequency liquid crystal optical [3] retarder, driven by an amplitude and frequency modulated voltage," Applied Physics Letters, 83(19), 3864-3866 (2003).
- [4] X.-W. Lin, W. Hu, X.-K. Hu et al., "Fast response dual-frequency liquid crystal switch with photo-patterned alignments," Optics Letters, 37(17), 3627-3629 (2012).
- W. Duan, P. Chen, B.-Y. Wei et al., "Fast-response and high-efficiency optical switch based on dual-frequency [5] liquid crystal polarization grating," Optical Materials Express, 6(2), 597-602 (2016).
- O. Melnyk, Y. Garbovskiy, D. Bueno-Baques et al., "Electro-optical switching of dual-frequency nematic liquid [6]
- crystals: Regimes of thin and thick cells," Crystals, 9(6), 314 (2019). B.-X. Li, R.-L. Xiao, S. Paladugu *et al.*, "Dye-doped dual-frequency nematic cells as fast-switching polarization-[7] independent shutters," Optics Express, 27(4), 3861-3866 (2019).
- [8] D. Węgłowska, M. Czerwiński, P. Kula et al., "Fast-response halogenated 4-alkyl-4"-cyano-p-terphenyls as dual frequency addressing nematics," Fluid Phase Equilibria, 522, 112770 (2020).

- [9] W. B. Jung, H. S. Jeong, H. J. Jeon *et al.*, "Polymer-Layer-Free Alignment for Fast Switching Nematic Liquid Crystals by Multifunctional Nanostructured Substrate," Advanced Materials, 27(42), 6760-6766 (2015).
- [10] J.-W. Kim, T.-H. Choi, and T.-H. Yoon, "Fast switching of nematic liquid crystals over a wide temperature range using a vertical bias electric field," Applied Optics, 53(26), 5856-5859 (2014).
- [11] M.-J. Cho, H.-G. Park, H.-C. Jeong *et al.*, "Superior fast switching of liquid crystal devices using graphene quantum dots," Liquid Crystals, 41(6), 761-767 (2014).
- [12] V. Borshch, S. V. Shiyanovskii, and O. D. Lavrentovich, "Nanosecond electro-optic switching of a liquid crystal," Physical review letters, 111(10), 107802 (2013).
- [13] B.-X. Li, V. Borshch, S. V. Shiyanovskii *et al.*, "Electro-optic switching of dielectrically negative nematic through nanosecond electric modification of order parameter," Applied Physics Letters, 104(20), (2014).
- [14] V. Borshch, S. V. Shiyanovskii, B.-X. Li *et al.*, "Nanosecond electro-optics of a nematic liquid crystal with negative dielectric anisotropy," Physical Review E, 90(6), 062504 (2014).
- [15] B.-X. Li, V. Borshch, D. Shiyanovskij *et al.*, "Nanosecond electric modification of order parameter in nematic and isotropic phases of materials with negative and positive dielectric anisotropy." 9384, 117-126.
- [16] B.-X. Li, V. Borshch, H. Wang *et al.*, "Enhanced nanosecond electro-optic effect in isotropic and nematic phases of dielectrically negative nematics doped by strongly polar additive," Journal of Molecular Liquids, 267, 450-455 (2018).
- [17] L.-Y. Sun, X.-Y. Wang, J.-H. Chen *et al.*, "Electrical modification of order parameters and director fluctuations in a dielectrically negative nematic doped with a positive additive," Journal of Molecular Liquids, 363, 119843 (2022).
- [18] B.-X. Li, G. Babakhanova, R.-L. Xiao *et al.*, "Microsecond electro-optic switching of nematic liquid crystals with giant dielectric anisotropy," Physical Review Applied, 12(2), 024005 (2019).
- [19] R. J. Mandle, S. J. Cowling, and J. W. Goodby, "A nematic to nematic transformation exhibited by a rod-like liquid crystal," Physical Chemistry Chemical Physics, 19(18), 11429-11435 (2017).
- [20] H. Nishikawa, K. Shiroshita, H. Higuchi *et al.*, "A fluid liquid-crystal material with highly polar order," Advanced materials, 29(43), 1702354 (2017).
- [21] A. Mertelj, L. Cmok, N. Sebastián et al., "Splay nematic phase," Physical Review X, 8(4), 041025 (2018).
- [22] N. Sebastián, L. Cmok, R. J. Mandle *et al.*, "Ferroelectric-ferroelastic phase transition in a nematic liquid crystal," Physical review letters, 124(3), 037801 (2020).
- [23] X. Chen, E. Korblova, D. Dong *et al.*, "First-principles experimental demonstration of ferroelectricity in a thermotropic nematic liquid crystal: Polar domains and striking electro-optics," Proceedings of the National Academy of Sciences, 117(25), 14021-14031 (2020).
- [24] A. Manabe, M. Bremer, and M. Kraska, "Ferroelectric nematic phase at and below room temperature," Liquid Crystals, 48(8), 1079-1086 (2021).
- [25] A. Adaka, M. Rajabi, N. Haputhantrige *et al.*, "Dielectric Properties of a Ferroelectric Nematic Material: Quantitative Test of the Polarization-Capacitance Goldstone Mode," Physical Review Letters, 133(3), 038101 (2024).
- [26] J.-S. Yu, J. H. Lee, J.-Y. Lee *et al.*, "Alignment properties of a ferroelectric nematic liquid crystal on the rubbed substrates," Soft Matter, 19(13), 2446-2453 (2023).
- [27] B. Basnet, M. Rajabi, H. Wang *et al.*, "Soliton walls paired by polar surface interactions in a ferroelectric nematic liquid crystal," Nature Communications, 13(1), 3932 (2022).
- [28] S.-T. Wu, A. M. Lackner, and U. Efron, "Optimal operation temperature of liquid crystal modulators," Applied optics, 26(16), 3441-3445 (1987).
- [29] S.-T. Wu, M. Neubert, S. Keast *et al.*, "Wide nematic range alkenyl diphenyldiacetylene liquid crystals," Applied Physics Letters, 77(7), 957-959 (2000).
- [30] B. Malraison, Y. Poggi, and E. Guyon, "Nematic liquid crystals in high magnetic field: Quenching of the transverse fluctuations," Physical Review A, 21(3), 1012 (1980).
- [31] D. Dunmur, T. Waterworth, and P. Palffy-Muhoray, "Electric field induced birefringence in nematic liquid crystal films: evidence for wall quenching of director fluctuations," Molecular Crystals And Liquid Crystals, 124(1), 73-88 (1985).
- [32] Y. Yin, S. V. Shiyanovskii, A. Golovin *et al.*, "Dielectric torque and orientation dynamics of liquid crystals with dielectric dispersion," Physical Review Letters, 95(8), 087801 (2005).
- [33] S. V. Shiyanovskii, and O. D. Lavrentovich, "Dielectric relaxation and memory effects in nematic liquid crystals," Liquid Crystals, 37(6-7), 737-745 (2010).